Int. J. Appl. Math. Comput. Sci., 2014, Vol. 24, No. 3, 599–609
DOI: 10.2478/amcs-2014-0043

A SIMULTANEOUS LOCALIZATION AND TRACKING METHOD FOR A WORM TRACKING SYSTEM

MATEUSZ KOWALSKI *, PIOTR KACZMAREK *, RAFAŁ KABACIŃSKI *,
MIESZKO MATUSZCZAK *, KAMIL TRANBOWICZ *, ROBERT SOBKOWIAK **

* Institute of Control and Information Engineering
Poznań University of Technology, ul. Piotrowo 3a, 60-965 Poznań, Poland
e-mail: mateusz.m.kowalski@doctorate.put.poznan.pl

**Department of Cell Biology, Institute of Experimental Biology
Adam Mickiewicz University, ul. Umultowska 89, 61-614 Poznań, Poland
e-mail: robsob@amu.edu.pl

The idea of worm tracking refers to the path analysis of *Caenorhabditis elegans* nematodes and is an important tool in neurobiology which helps to describe their behavior. Knowledge about nematode behavior can be applied as a model to study the physiological addiction process or other nervous system processes in animals and humans. Tracking is performed by using a special manipulator positioning a microscope with a camera over a dish with an observed individual. In the paper, the accuracy of a nematode's trajectory reconstruction is investigated. Special attention is paid to analyzing errors that occurred during the microscope displacements. Two sources of errors in the trajectory reconstruction are shown. One is due to the difficulty in accurately measuring the microscope shift, the other is due to a nematode displacement during the microscope movement. A new method that increases path reconstruction accuracy based only on the registered sequence of images is proposed. The method Simultaneously Localizes And Tracks (SLAT) the nematodes, and is robust to the positioning system displacement errors. The proposed method predicts the nematode position by using NonParametric Regression (NPR). In addition, two other methods of the SLAT problem are implemented to evaluate the NPR method. The first consists in ignoring the nematode displacement during microscope movement, and the second is based on a Kalman filter. The results suggest that the SLAT method based on nonparametric regression gives the most promising results and decreases the error of trajectory reconstruction by 25% compared with reconstruction based on data from the positioning system.

Keywords: *Caenorhabditis elegans* behavior, worm tracking, computer vision, image processing, feature extraction.

1. Introduction

The *Caenorhabditis elegans* nematode as a model organism is a valuable object of many medical and biological studies (Rankin, 2002). This is because it has a fully sequenced genome (CESC, 1988), a well-known neurological system with a constant number of cells (White *et al*., 1986) and a rapid life cycle, and allows easy genetic manipulations (Jorgensen and Mango, 2002). The great amount of research using *C. elegans* and the WormBook.org open access platform for knowledge exchange has increased its usefulness even more.

Many nervous system diseases such as Parkinson's syndrome (Nass *et al*., 2001), Alzheimer's disease (Wu *et al*., 2006) and Duchenne muscular dystrophy (Ségalat *et al*., 2005) are studied with the use of this nematode species. In addition, reactions to different substances that affect the human nervous system can be investigated. Nematodes can react even to very small amounts of various substances. *C. elegans* behavior is studied in the context of their locomotion, i.e., chosen directions, velocity, problems with coordination, etc. (Baek *et al*., 2002; Sobkowiak *et al*., 2011; Pierce-Shimomura *et al*., 1999; Gray *et al*., 2005), egg laying (Waggoner *et al*., 1998; Hardaker *et al*., 2001) and social behavior (de Bono and Bargmann, 1998).

This paper is focused on issues related to analyzing *C. elegans* locomotion behavior. Further, this aspect is called worm tracking.

1.1. Nematode locomotion behavior. In neurobiology studies, worm tracking seems to be a new field of knowledge. This type of research has been conducted since the 1990s (de Bono and Bargmann, 1998; Pierce-Shimomura *et al*., 1999), when technical solutions allowed automated worm tracking, registration of long sequences of images taken with high magnification, and analysis of large data sets.

Research on nematode behavior in the context of locomotion includes analysis of global parameters such as the path, chosen directions, speed or angular velocity (Pierce-Shimomura *et al*., 1999), and local parameters such as postures taken by nematodes or their shapes during movement. Currently, many studies (Baek *et al*., 2002; Geng *et al*., 2004; Feng *et al*., 2004) are focused on methods for determining the type of mutation in the *C. elegans* genome based on analyzing its locomotion.

1.2. Worm tracking systems. Statistical significance in research on *C. elegans* locomotion requires automated tracking systems. Depending on biological aspects, two main categories can be distinguished: systems that track multiple animals and those that track a single worm over a long period (Husson *et al*., 2012). When a single worm is tracked over a long time interval, an appropriate scene selecting and registering method is important due to the nematode's size and motility. The maximum pixel size should be lower than 24 μm in order to prevent the worm from vanishing (Husson *et al*., 2012). However, during long-term observations with high magnification, the nematode can leave the scene.

A number of worm tracking system configurations have been implemented:

- Using a high-resolution camera (2352×1728) and an immobile dish (Ramot *et al*., 2008; Roussel *et al*., 2007). The drawback of this approach is a rather small observation area. It is usually applied to multiple worm tracking systems.

- Using immobile microscope with a camera and a dish placed on a motorized stage (Feng *et al*., 2004; Pierce-Shimomura *et al*., 1999; Hoshi and Shingai, 2006). The drawbacks of this solution are dish movements and mechanical vibrations transmitted to the dish that can agitate nematodes (Husson *et al*., 2012). Nevertheless, this approach is popular due to the simplicity and easy construction because of the low-moving mass.

- Using a mobile microscope with a camera and an immobile dish (Baek *et al*., 2002). This solution can track a single nematode over a long period; however, its disadvantage is a high price because of the need for precise actuators (MRC-LMB, 2012).

1.3. Problem statement. Systems that track nematodes correct their position only when the worm leaves a predefined area in the image (Baek *et al*., 2002; Pierce-Shimomura *et al*., 1999; Hoshi and Shingai, 2006). In this case, the nematode's path is computed from its movements recorded on the sequence of images and the registered device movements. In this approach, the measurement accuracy might be decreased by

- the synchronization between positioning system displacement recordings and nematode displacements computed from subsequent image frames,

- an error determining the pixel size, and

- an error determining positioning the system displacement.

The last issue is significantly influential, especially in systems without encoders. In such systems, the manipulator displacement can be estimated only by assuming a fixed step size of the device and registering the time when the movement occurs.

Detecting a positioning system displacement based on the feature matching method applied to consecutive frames might fail as the environments in which *C. elegans* are tracked are usually poor and homogeneous. Therefore, matching consecutive images is difficult. The first solution to this problem involves introducing artificial landmarks into the nematode environment. However, they might influence its behavior as they are physical obstacles or may become attractants. The second solution consist in using markers attached to the bottom of the dish (e.g., a marker grid). In this case, the image segmentation process is technically difficult because the depth of the field of the microscope is very narrow while the nematode and markers are located at different distances from the camera. Moreover, taking into account the nematode sensitivity to the temperature and the light means that the markers might affect the nematode behavior.

In this article, the problem of reconstructing the path based only on a sequence of images, while prior knowledge about the positioning system displacements is not required, is stated. Analogously to the Simultaneous Localization And Map building (SLAM) problem (Bączyk and Kasiński, 2010; Skrzypczyński, 2009), it is called Simultaneous Localization And Tracking (SLAT). Solving it consists in estimating the nematode's locomotion and positioning system displacements from the sequence of images where the only characteristic point is a moving nematode.

A new method for the SLAT problem based on Non-Parametric Regression (NPR) is proposed. Two other methods that can be applied to solve the SLAT problem were implemented to evaluate the NPR method. One consist in ignoring the nematode displacement during the microscope movement, and the other is based on a Kalman filter.

The ground truth path was extracted from images recorded with the use of markers attached to the bottom of the dish. Markers can be used, as analyzing nematode behavior is not the objective of this research. In addition, the statistics of the positioning system step length were provided to obtain a reference for further evaluation of NPR and other methods.

2. Materials and methods

2.1. Strains and culture methods. All tests were performed on the wild-type Bristol N2 strain of *C. elegans* obtained from the Caenorhabditis Genetics Center (CGC) at the University of Minnesota (Duluth, MN, USA). Standard methods were used for maintaining and manipulating strains (Stiernagle, 2006). Nematodes were maintained at 22°C on 5 cm NGM agar plates seeded with *Escherichia coli* (OP50). The young adult worm was manually picked off the maintenance plate and placed into 1 μL of water, which was applied to the center of the testing plate. This avoids scratching the agar surface (important for obtaining high-contrast videos). The worm was initially trapped in the drop because *C. elegans* cannot break the surface tension of the water. Temporary worm immobilization in the drop of water gave time to set up the equipment. After the water had evaporated or had been soaked up, the tracking procedure could start.

2.2. Acquisition system. The acquisition system is a custom made, two-dimensional Cartesian coordinate robot with a microscope, and a dish with nematodes placed on a separate stand. Figure 1 presents the assembled device consisting of

- a fixed base on four legs with adjustable height,
- a moving carriage (the y-axis) on which the gate is mounted, and
- a gate, with a moving carriage (the x-axis) with a microscope attached.

The work plane of the device is 100 mm wide (the y-axis) and 100 mm long (the x-axis). This allows worms to be tracked for a long period of time in 10 cm diameter dishes. On both the axes, the carriages of the positioning system fitted with linear bearings move on precision shafts. They are powered by modules, consisting of stepper motors connected by coupling with lead screws and nuts attached to the carriages. The system uses two-phase bipolar stepper motors controlled by a PC. Movement commands can be generated automatically in response to the results of the image processing algorithms of the vision system, or by the human operator. To improve the image acquisition conditions, a special stand with lighting for dishes with nematodes was built. In this way, the sample is illuminated uniformly with the light of an adequate color temperature. The positioning system speed is up to 1 mm/s in the direction of each axis, which exceeds the maximum locomotion velocity of nematodes. The device's basic step length is 0.5 mm. Depending on the selected magnification, recordings can be done at various scales. For a given step length, the area of an observed scene smaller than 1.92×1.44 mm might cause after the system shift only part of the nematode's body to be visible.

2.3. Image acquisition and processing. Videos were recorded at the rate of 10 fps, and the resolution was 640×480. Videos were saved in the AVI format and processed in the Matlab environment.

During the experiments, single, freely moving nematodes were observed. To calculate the ground truth trajectory, a grid of markers was used. It consisted of a matrix of black dots with a center-to-center distance of 1.55 mm. The dots were printed on a self-adhesive foil with a high-resolution ink-jet printer. This foil was attached to the bottom of the dish. Images were registered with a pixel size of 10 μm, which ensured that at least 12 markers were visible at each frame.

The difference in the distance from the camera to the nematode's plane and the markers' plane resulted in problems with obtaining them in focus. Moreover, it led to the extension of the gray-scale of the recorded image with black markers, a dark nematode and a bright background. The presence of the marker grid therefore required a complex method of nematode segmentation and a dedicated method for marker separation.

The reference markers were extracted from the image with the global thresholding method, with the threshold obtained using the Otsu method (Otsu, 1979) that corresponds to changes between nodes 2 and 3a in Fig. 2(b).

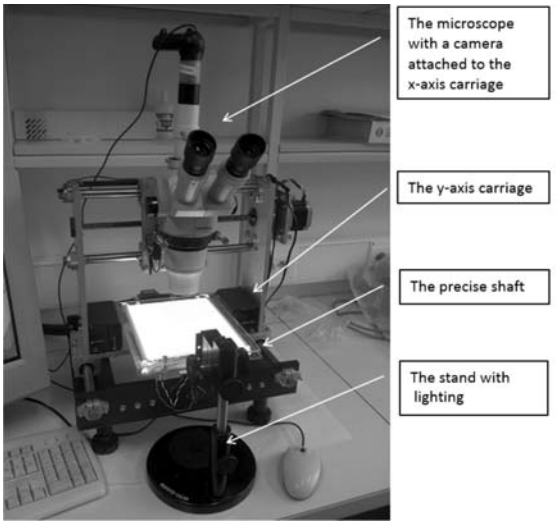

Fig. 1. Assembled acquisition system.

A sample image showing binarization results is presented in Fig. 2(c). Each marker was described by Cartesian coordinates calculated from the center of mass of the corresponding blob (Fig. 2(b), between nodes 3a and 4a).

Nematodes were extracted from the image in the following steps:

1. First, the grayscale image was binarized (Fig. 2(b), between nodes 2 and 3b) using the adaptive thresholding method (Perez and Gonzalez, 1987), in which the threshold was calculated as the mean value of pixels under a square mask of size 50 px.

2. Next, the XOR operation between the binary obtained in previous step and the binary image with extracted markers was applied (Fig. 2(b), between nodes 2 and 3b). In Fig. 2(d), the image after that step is shown.

3. Finally, the center of mass of the largest blob was recorded as the nematode position (Fig. 2(b), between nodes 3b and 4b).

2.4. Camera calibration. The single parameter division camera distortion model was used (Fitzgibbon, 2001). The camera calibration was performed by using a marker grid and constrained nonlinear minimization (Byrd *et al.*, 2000), where the objective function was defined:

$$\mathrm{err} = \sum \mathrm{err}^2_{\mathrm{linearity}} + k \cdot \sigma^2_{\mathrm{distance}}, \tag{1}$$

with $\mathrm{err}_{\mathrm{linearity}}$ being the linearity error calculated for markers located in a particular row or column, $\sigma^2_{\mathrm{distance}}$ being the variance of neighboring marker distances, and k being a weight used to ensure the same contribution of the factors to the objective function value. The procedure decreased the radial and perspective distortions. The standard calibration procedures estimated the camera matrix, and the camera distortion was impossible due to a constant orientation of the microscope table.

2.5. Ground truth extraction. The ground truth trajectories were determined by using the grid of markers. The position of the i-th marker on the n-th frame is denoted as

$$M_i(n) = [x_{mi}(n), y_{mi}(n)], \tag{2}$$

where $i = 1, 2, 3, \ldots, N(n)$, n is the index of the frame, $N(n)$ is the number of markers detected on the n-th frame, and x_{mi},y_{mi} are coordinates of a single marker.

For each frame, the position of the i-th marker in relation to the nematode was calculated and denoted as the vector

$$V_i(n) = M_i(n) - O(n), \tag{3}$$

where $O(n) = [x(n), y(n)]$ is the nematode's center of mass position in the n-th image frame.

Then the markers' positions in two subsequent frames were compared by calculating the Euclidean distance:

$$D_{ij}(n) = \|V_i(n) - V_j(n-1)\|. \tag{4}$$

Marker matching on subsequent frames was performed by looking for a pair of markers $M_k(n)$ (in the n-th frame) and $M_l(n-1)$ (in the $n-1$ frame) whose distance in relation to the nematode was not greater than a threshold ε. The threshold was assumed to be 40 px (400 μm), which corresponded to the maximum nematode displacement of 15 px (150 μm) in six subsequent frames and the maximum segmentation error of 25 px (250 μm) influencing the center of mass position. This error might occur when more than 25% of the nematode's body is not properly extracted. If different numbers of markers were detected on matched frames, the following matching conditions had to be fulfilled:

$$D_{kl}(n) = \begin{cases} \min\limits_{j}([D(n)]_{kj}) & \text{if} \quad N(n) \le N(n-1), \\ \min\limits_{i}([D(n)]_{il}) & \text{if} \quad \text{otherwise}, \end{cases}$$
$$D_{kl}(n) < \varepsilon. \tag{5}$$

This method matches markers even if the positions of the nematode and the microscope change from frame to frame (Fig. 3). The displacement vector $T(n)$ is calculated from two subsequent frames (i.e., for n and $(n-1)$) as the averaged displacement vector of all matched markers.

For each newly observed marker, a unique label is assigned based on its neighbors' labels and positions. The maximum step size ensures that, after the system shifts, at least six markers from the previous frame are visible in the current frame. This reconstructs the global position of new markers.

The absolute position of the nematode in the current frame was calculated as

$$P_{GT}(n) = O(n) - \sum_{k=2}^{n} T(k), \tag{6}$$

where $P_{GT} = (x_{GT}, y_{GT})$ will be further assumed to be the ground truth path for the markerless tracking algorithm. The block diagram of the algorithm used to acquire the reference nematode path is presented in Fig. 2(b).

2.6. Path correction method. As mentioned in Section 1.3, the marker-based algorithm reconstructs the accurate nematode path, but it cannot be used in research on nematode locomotion because the markers significantly complicate nematode extraction from the image and may influence the nematode behavior.

For a system with a known control sequence of positioning manipulator shifts, the nematode's absolute position can be calculated assuming a fixed step size. However, it can generate errors due to a step size variation, a

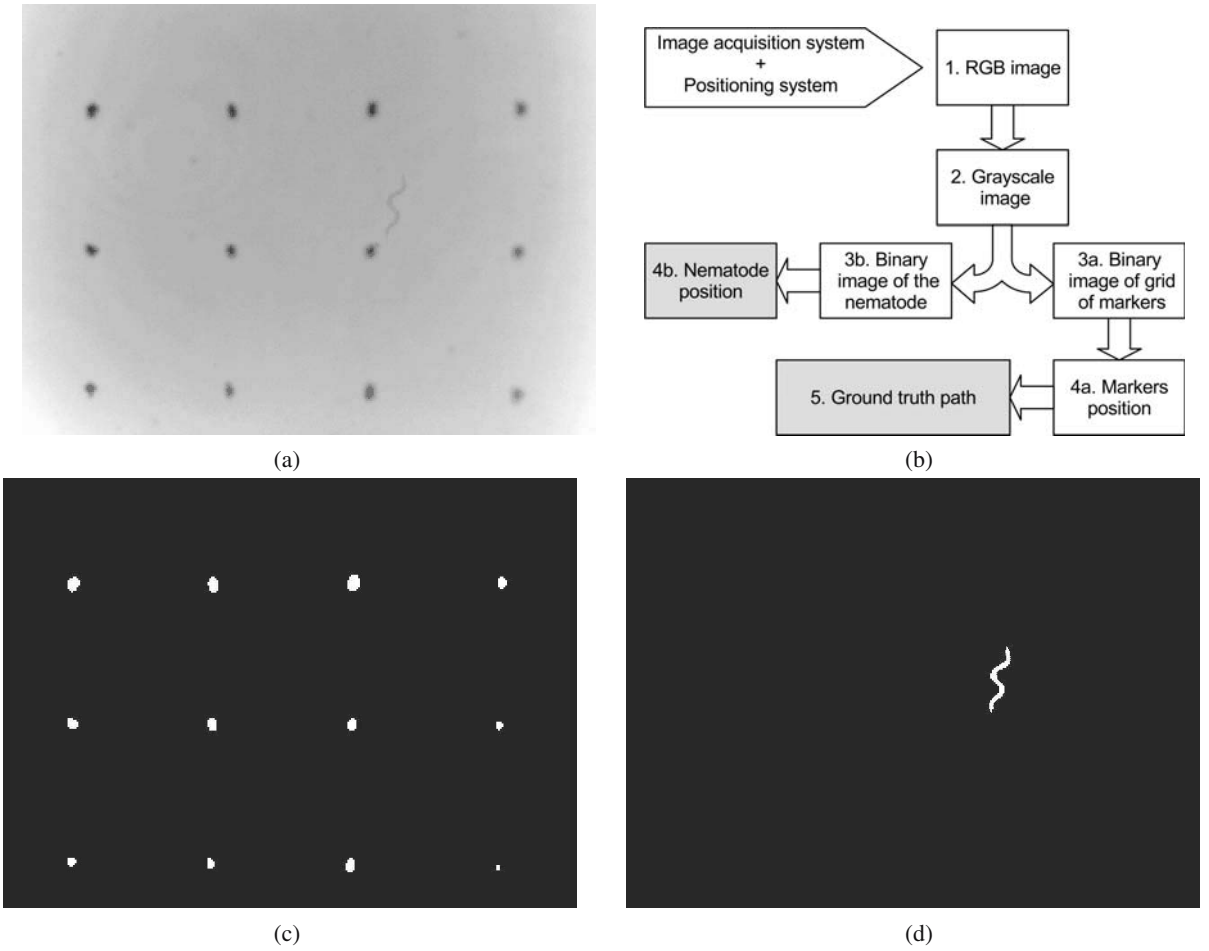

Fig. 2. Nematode and markers extraction: original image in grayscale (a), block diagram of the algorithm used to acquire the reference nematode track (b), markers extracted with the global thresholding method with a threshold of 20% grayscale (c), nematode extracted with the adaptive thresholding method (with mask 50×50 px) after morphological closing (d).

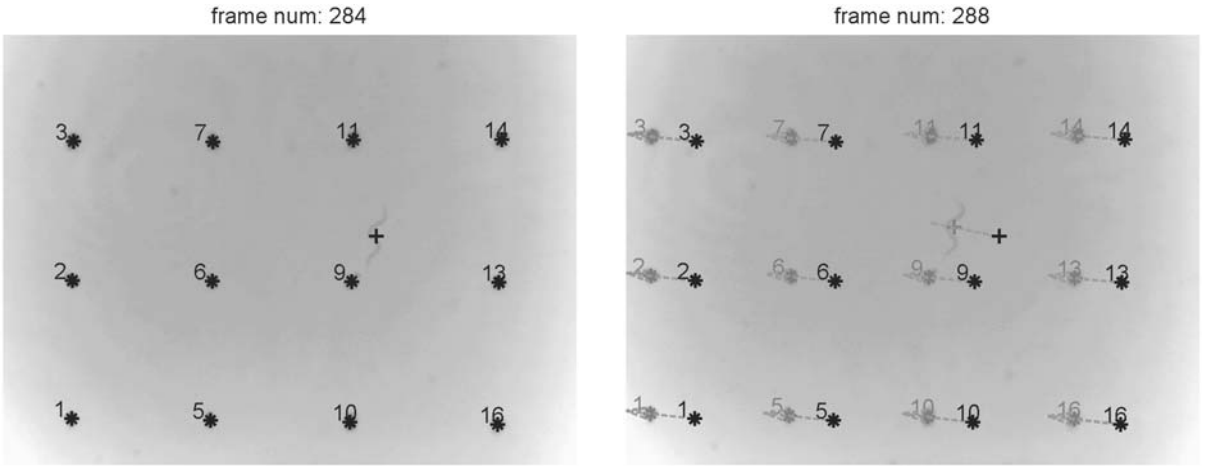

Fig. 3. Results for the marker-based tracking algorithm: frame with detected markers denoted with '*' and the nematode position denoted with '+' (a), next frame with detected and matched markers after the positioning system shift (b). The markers and nematode positions corresponding to the previous frame are in black.

step loss, accidental shifts, differences in the orientation of the image coordinates and the positioning system.

The simplest solution to markerless tracking, which does not require information about the positioning system control sequence, omits nematode displacements during positioning system movements. It can be implemented by assuming that, on the frame before and after the movement, the nematode's center of mass is in the same place. The path acquired in this way is called the zero-path and is denoted by $P_0 = (x_0, y_0)$. However, P_0 is easy to calculate; it is evident that neglecting the nematode displacement during positioning system movements generates an error cumulating in time. In our work, localization and tracking accuracy was increased by using nonparametric regression (de Boor, 1978) to predict the nematode position when positioning system shift occurred.

The trajectory is denoted as

$$\tilde{P}(n) = (\tilde{s}_x(n), \tilde{s}_y(n)), \tag{7}$$

where the coordinates $\tilde{s}_x(n)$ and $\tilde{s}_y(n)$ are estimated using nonparametric regression, with the estimated values of the nematode position in the n-th frame defined as a cubic spline function

$$\tilde{s}_x(n) = P_x(n) + \sum_{k \in K} \beta_{p+1}(n-k)_+^p, \tag{8}$$

where β is a polynomial coefficient, K is a set of spline knots and P_x denotes an arbitrary p-th degree ($p = 3$) polynomial while $(n-k)_+$ is zero for $n \leq k$ and $n-k$ for $n > k$, $\tilde{s}_y(n)$ is defined analogously to $\tilde{s}_x(n)$.

The coefficients of $\tilde{s}_x(n)$ are determined by minimizing the following criterion:

$$\lambda \sum_i (x(i) - \tilde{s}_x(i))^2 + (1-\lambda) \int \left(\frac{\mathrm{d}^2 \tilde{s}_x(t)}{\mathrm{d}t^2} \right)^2 \mathrm{d}t, \tag{9}$$

where λ is a smoothing parameter. When λ is equal to 1, the solution will be a cubic spline that almost interpolates the data; decreasing values of λ render increasingly smooth approximations and decrease spline oscillations. Since the wriggle of nematodes generates path oscillations of the center of mass, in order to reduce them, λ was set to 0.07, which was determined as the optimal value.

The path reconstruction algorithm consists of the following steps:

1. For each frame n >3, the predicted position of the nematode on the n-th frame was approximated from the spline function for the $(n-1)$-th frame. It is denoted as
$$\hat{P}(n) = \tilde{P}(n|n-1). \tag{10}$$
2. The difference between the predicted and the recorded nematode position is calculated as
$$\Delta(n) = \|O(n) - \hat{P}(n)\|. \tag{11}$$
3. If $\Delta(n) > \delta$, a positioning system movement is detected and the estimated value $\hat{P}(n)$ of the nematode position is assumed instead of the measured position $O(n)$. The threshold $\delta = 275$ μm was calculated assuming that the maximum nematode displacement from frame to frame is 2.5 px (25 μm) and the maximum segmentation error is 25 px (250 μm). The path reconstructed in this way, $\tilde{P}$, is further called the s-path.

2.7. Kalman filter. To compare the NPR method's accuracy, a Kalman filter for a second-order model (Kalman, 1960) was implemented. The filter was applied separately to estimate the position in the x and y directions. The discrete model state space equation is defined as

$$\underline{x}_k = A\underline{x}_{k-1} + B \cdot u_{k-1} + w_k, \tag{12}$$

$$A = \begin{bmatrix} 1 & \mathrm{d}t \\ 0 & 1 \end{bmatrix}, \quad B = \begin{bmatrix} \frac{\mathrm{d}t^2}{2} \\ \mathrm{d}t \end{bmatrix} \tag{13}$$

The input of the system is the acceleration in a particular direction; the output is the object position. The input signal (nematode acceleration) is unknown and was assumed to have a normal distribution $w_k \sim N(0, Q)$. The process noise covariance matrix was defined as

$$Q = B \cdot B^T \cdot \sigma_{\mathrm{acc}}^2 \tag{14}$$

where σ_{acc} is the variance of the observed nematode acceleration which was estimated from the recorded signal.

Analogously to the NPR method, it was assumed that the nematode relative displacement in periods without positioning system movements can be measured unambiguously. Therefore, the observation noise was assumed to be much smaller than process noise and was defined as

$$v_k \sim N\left(0, 0.01 \cdot \frac{\mathrm{d}t^2}{2} \sigma_{\mathrm{acc}}^2\right). \tag{15}$$

The nematode tracking algorithm was analogous to tracking with the NPR method, except that the nematode position during positioning system movements was taken from Kalman filter estimates. The path obtained in this way was denoted as P_K.

2.8. Comparison of the accuracy of the methods. The accuracy of each method was determined by comparing the path obtained by this method with the ground truth path. For a certain reconstructed path (P), the cumulative displacement error (DE) was computed as the Euclidean distance

$$DE(P, i) = d(P_{GT}(i), P(i)), \tag{16}$$

where i denotes the index of the frame.

According to the prior assumption, the localization error is generated only during positioning system shifts. Thus, the accuracy of NPR can be compared with other methods in terms of a single shift of the positioning system. The accuracy was calculated as follows:

1. For each positioning system shift, the Shift Error (SE) was calculated as

$$SE(P,k) = DE(P,N_k) - DE(P,N_{k-1}), \quad (17)$$

where N_k is the number of the first frame after the k-th shift.

2. The chi-square goodness-of-fit test of the default H_0 hypothesis that the data in vector $SE(P,.)$ are a random sample from a normal distribution with mean and variance estimated from $SE(P,.)$ was evaluated with a significance level 0.05.

3. If the H_0 hypothesis was not rejected, the error distribution is assumed to be $\sim N(\overline{SE}, \sigma_{SE})$ and the method accuracy at $p = 0.95$ is

$$\Delta = \pm(|\overline{SE}| + 2\sigma_{SE}). \quad (18)$$

Finally, to compare the accuracy improvement given by NPR and other methods, the Performance Ratio (PR) was calculated as the current method accuracy (Δ) in relation to the accuracy of a single step of the positioning system (Δ_{fix}),

$$PR = \frac{\Delta}{\Delta_{P_{\text{fix}}}}. \quad (19)$$

3. Experiments and results

In this study, a 15-minute recording with a single freely moving nematode was used. Within this period, 132 positioning system shifts were performed through manual control to prevent the nematode from leaving the observed area. The system had to be controlled manually due to the use of the marker grid, which required a more complex algorithm of the nematode and markers extraction (Section 2.3). The automated control methods turned out to generate errors in extreme situations when motion-blurred images occurred during system shifts. This prevented the use of an automated system. The raw recordings contained image frames that were blurred by positioning system movements; therefore, they could not be used for the analysis and were excluded. The number of rejected frames did not exceed 9.5%, and no more than 6 consecutive frames were removed from the movie.

Sample results for the marker matching procedure are presented in Fig. 3. The marker matching method successfully reconstructed the ground truth path and positioning system displacements during the tracking procedure. The results of nematode position recordings (P_{GT} path) were supervised to prevent any errors.

In the material recorded with the use of markers, all typical sets of nematodes maneuvers were noticed. Therefore, it can be assumed that the observed nematode behavior was not significantly influenced by the markers' grid.

The expected step length of the positioning system was 500 μm (50 px) and was determined by the system mechanical properties. The measured average step size obtained from the analysis of marker grid displacements was 46.1±9.7 px (461±97 μm) with the confidence level $p = 0.95$. The high variation in the positioning system step might be due to the following reasons: coupling and lead screw backslash, friction between the screw and nut, and misalignment of leading shafts.

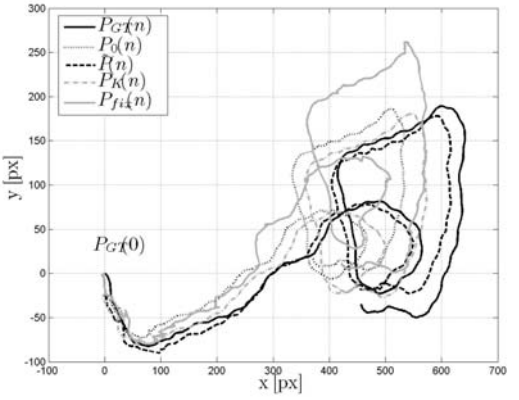

(a)

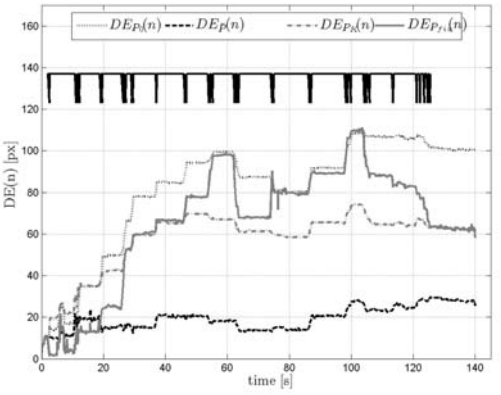

(b)

Fig. 4. Sample ground truth path (P_{GT}), zero-path (P_0), s-path ($\tilde{P}$), Kalman-filter-based path (P_K) and fixed step size path (P_{fix}) (a), time-evolution of the distance error (DE) for P_{GT}, P_0, $\tilde{P}$, P_K and P_{fix} paths (b). The vertical lines in the upper part of the plot denote the positioning system shifts.

The calculated step size was used to reconstruct the nematode position based on the known control sequence

of the positioning system. This trajectory is further denoted as the fixed step size path P_{fix}.

To compare the accuracy of the methods, the Shift Error (SE) and the method accuracy (Δ) were calculated. The error was assumed to have a normal distribution, as the null hypothesis was not falsified in the χ^2 test. The variance of the positioning system step was assumed to be the reference value to evaluate the accuracy of the proposed methods. The results are summarized in Table 1. The last column presents the method performance ratio. The analysis of the table contents reveals that the accuracy of the single step by using the $\tilde{P}$ method is about 30% better then the Kalman-filter-based method and fixed step size approaches.

In Fig. 4(a), the computed representative ground truth path (P_{GT}) and the NPR method s-path ($\tilde{P}$) are presented. In addition, the zero path (P_0), P_K and the P_{fix} path, which was reconstructed based on the known positioning system shift and a constant step size, are shown in this figure. The presented path was recorded during a period of 2 minutes 20 seconds. The calculated length of the P_{GT} path was 1594 px (19430 μm). At the same time, the positioning system performed 20 steps in the x-direction and 22 steps in the y-direction.

In Fig. 4(b), the displacement error for all paths except the s-path increased abruptly in the first minute of the recording, when the nematode moved along a straight line. Next, the errors stopped increasing because the nematode preformed two wide loops. At the end of the path, the displacement error for $\tilde{P}$, P_0, P_K and P_{fix} reached respectively 24.8 px, 99.8 px, 61.8 px, and 58.2 px. The greater error was observed in the x-direction (Figs. 5(a) and (b)).

The path calculated by using the nonparametric regression method compared to P_0 revealed a better fit to the ground truth path. For the majority of positioning system displacements, during the course of residuals for the s-path small, rapidly vanishing peaks were observed (Figs. 5(c) and (d)).

4. Conclusions

In this paper, a self-constructed, low-cost worm tracking system was presented. It performs worm tracking on a Petri dish with a 10 cm diameter. The accuracy analysis revealed relatively large positioning errors. Thus, a path reconstructed based on data from the positioning system controller may be incorrect due to the fixed step-size assumption and mechanical system inaccuracy. Commercial systems dedicated to worm tracking purposes cost over 10 times more than the presented system. They are more precise and have declared repeatability. However, a majority of them still use the fixed step size assumption to estimate positions. Thus, faults and inaccuracy of the actuating system cannot be detected and its influence on trajectory reconstruction evaluated. Moreover, an additional source of inaccuracy might be the non-zero angle between the image coordinate system and the positioning system.

Table 1. Comparison of the methods' performance.

Method	$\overline{DE}$	σ_{DE}	Δ	Performance ratio (PR)
P_{fix}	0	4.87	9.73	1.00
$\tilde{P}$	1.08	3.10	7.28	1.33
P_K	2.33	3.49	9.31	1.04
P_0	2.33	5.61	13.54	0.72

The most important feature of the stated SLAT problem is the use of machine vision methods to compensate the positioning system inaccuracy. The results showed that the proposed NPR method could be successfully applied even when the positioning system displacement was unknown.

The prediction based on this method made it possible to obtain satisfactory results, and decrease the error compared with tracking on the basis of the fixed step size assumption (up to 1.3 times better). The proposed method reduced the influence of positioning system inaccuracy on the reconstructed path. The methods also reduced the errors influenced by vision system calibration and the transformation of the image coordinates to global coordinates during data fusion from the vision and positioning systems.

Moreover, the NPR method efficiently predicted worm positions in frames where they could not be extracted from the image and therefore significantly decreased errors compared with the zero path method (up to 1.8 times better). The analysis revealed that tracking accuracy could be enhanced by predicting nematode movement in frames that were distorted due to positioning system movement.

In addition, compared with the technique based on the Kalman filter, the NPR method reveals important advantages (up to 1.28 times better). Whenever the nematode moved along a straight line, the error in the case of the Kalman-filter-based method increased greatly (Figs. 4 and 5 for time intervals between 10 s and 50 s). This can be explained by nematode wriggle that generates oscillations of the center of mass resulting in a position estimation error during positioning system shifts. The difference in the accuracy between the NPR method and the Kalman filter can be explained based on model dynamics. The NPR method using cubic splines corresponds to third-order model dynamics and it better mimics velocity changes. The second-order model, used in the Kalman filter, cannot mimic oscillations of the center of mass and cannot predict velocity changes because the acceleration is not a state-space variable.

The results suggest that the proposed method is not

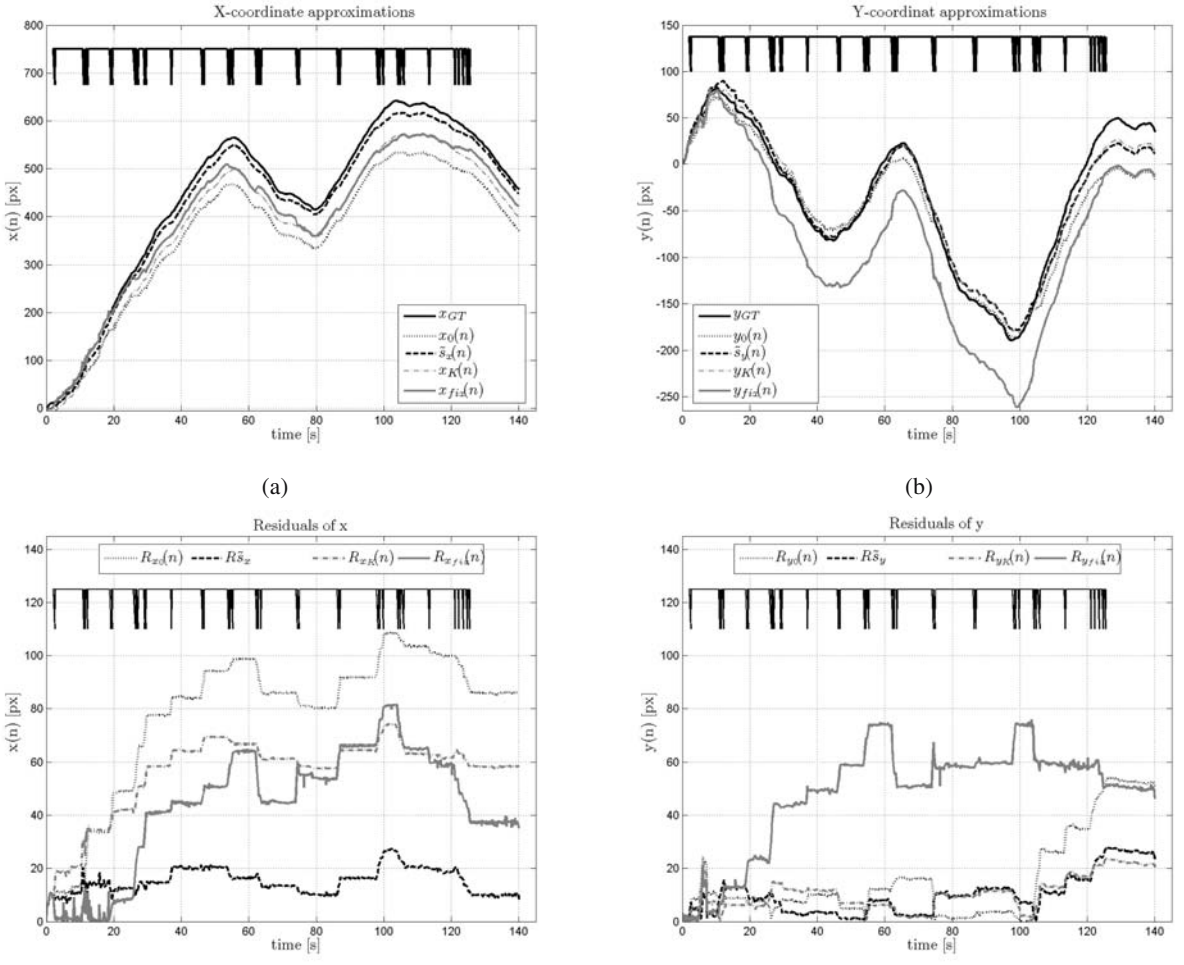

Fig. 5. Time evolution of the nematode path in the x and y directions, respectively (a) and (b), residuals of the P_0 and $\tilde{P}$, P_K, P_{fix} paths in the x and y directions, respectively (c) and (d). The vertical lines in the upper part of the subplots denote the positioning system shifts.

resistant to nematode-specific behavior such as a reversal occurring together with positioning system movements. The accuracy of the method can be improved by replacing the employed kinematic model of the center of mass, described by nonparametric regression or a Kalman filter, with another model reflecting the nematode's locomotion dynamics, wriggling and various atypical behaviors.

References

Bączyk, R. and Kasiński, A. (2010). Visual simultaneous localisation and map-building supported by structured landmarks, *International Journal of Applied Mathematics and Computer Science* **20**(2): 281–293, DOI: 10.2478/v10006-010-0021-7.

Baek, J.-H., Cosman, P., Feng, Z., Silver, J. and Schafer, W.R. (2002). Using machine vision to analyze and classify *Caenorhabditis elegans* behavioral phenotypes quantitatively, *Journal of Neuroscience Methods* **118**(1): 9–21.

Byrd, R., Gilbert, J.C. and Nocedal, J. (2000). A trust region method based on interior point techniques for nonlinear programming, *Mathematical Programming* **89**(1): 149–185.

CESC (1988). Genome sequence of the nematode *C. elegans*: A platform for investigating biology, *Science* **282**(5396): 2012–2018.

de Bono, M. and Bargmann, C.I. (1998). Natural variation in a neuropeptide Y receptor homolog modifies social behavior and food response in *C. elegans*, *Cell* **94**(5): 679–689.

de Boor, C. (1978). *A Practical Guide to Splines*, Springer, New York, NY.

Feng, Z., Cronin, C., Wittig, J., Sternberg, P. and Schafer, W. (2004). An imaging system for standardized quantitative analysis of *C. elegans* behavior, *BMC Bioinformatics* **5**(1): 115.

Fitzgibbon, A. (2001). Simultaneous linear estimation of multiple view geometry and lens distortion, *Proceedings of the 2001 IEEE Computer Society Conference on Computer Vision and Pattern Recognition, CVPR 2001, Kauai, HI, USA*, Vol. 1, pp. I–125–I–132.

Geng, W., Cosman, P., Berry, C., Feng, Z. and Schafer, W. R. (2004). Automatic tracking, feature extraction and classification of *C. elegans* phenotypes, *IEEE Transactions on Biomedical Engineering* **51**(10): 1811 –1820.

Gray, J.M., Hill, J.J. and Bargmann, C.I. (2005). A circuit for navigation in *Caenorhabditis elegans*, *Proceedings of the National Academy of Sciences of the United States of America* **102**(9): 3184–3191.

Hardaker, L.A., Singer, E., Kerr, R., Zhou, G. and Schafer, W.R. (2001). Serotonin modulates locomotory behavior and coordinates egg-laying and movement in *Caenorhabditis elegans*, *Journal of Neurobiology* **49**(4): 303–313.

Hoshi, K. and Shingai, R. (2006). Computer-driven automatic identification of locomotion states in *Caenorhabditis elegans*, *Journal of Neuroscience Methods* **157**(2): 355–363.

Husson, S.J., Costa, W.S., Schmitt, C. and Gottschalk, A. (2012). Keeping track of worm trackers, `http://www.wormbook.org/chapters/www_tracking/tracking.html`.

Jorgensen, E.M. and Mango, S.E. (2002). The art and design of genetic screens: *Caenorhabditis elegans*, *Nature Reviews Genetics* **3**(5): 356–369.

Kalman, R.E. (1960). A new approach to linear filtering and prediction problems, *Transactions of the ASME Journal of Basic Engineering D* **82**: 35–45.

MRC-LMB (2012). Part list for a single tracking unit, `http://www.mrc-lmb.cam.ac.uk/wormtracker/webcontent/TrackerUnitPartList.pdf`.

Nass, R., Miller III, D.M. and Blakely, R.D. (2001). *C. elegans*: A novel pharmacogenetic model to study Parkinson's disease, *Parkinsonism and Related Disorders* **7**(3): 185–191.

Otsu, N. (1979). A threshold selection method from gray-level histograms, *IEEE Transactions on Systems, Man, and Cybernetics* **9**(1): 62–66.

Perez, A. and Gonzalez, R.C. (1987). An iterative thresholding algorithm for image segmentation, *IEEE Transactions on Pattern Analysis And Machine Intelligence* **9**(6): 742–751.

Pierce-Shimomura, J.T., Morse, T.M. and Lockery, S.R. (1999). The fundamental role of pirouettes in *Caenorhabditis elegans* chemotaxis, *The Journal of Neuroscience* **19**(21): 9557–9569.

Ramot, D., Johnson, B.E., Berry, Jr, T.L., Carnell, L. and Goodman, M. B. (2008). The parallel worm tracker: A platform for measuring average speed and drug-induced paralysis in nematodes, *PLoS ONE* **3**(5): e2208.

Rankin, C. H. (2002). From gene to identified neuron to behaviour in *Caenorhabditis elegans*, *Nature Reviews Genetics* **3**(8): 622–630.

Roussel, N., Morton, C., Finger, F. and Roysam, B. (2007). A computational model for *C. elegans* locomotory behavior: Application to multiworm tracking, *IEEE Transactions on Biomedical Engineering* **54**(10): 1786–1797.

Ségalat, L., Grisoni, K., Archer, J., Vargas, C., Bertrand, A. and Anderson, J. (2005). Capon expression in skeletal muscle is regulated by position, repair, NOS activity, and dystrophy, *Experimental Cell Research* **302**(2): 170–179.

Skrzypczyński, P. (2009). Simultaneous localization and mapping: A feature-based probabilistic approach, *International Journal of Applied Mathematics and Computer Science* **19**(4): 575–588, DOI: 10.2478/v10006-009-0045-z.

Sobkowiak, R., Kowalski, M. and Lesicki, A. (2011). Concentration- and time-dependent behavioral changes in *Caenorhabditis elegans* after exposure to nicotine, *Pharmacology Biochemistry and Behavior* **99**(3): 365–370.

Stiernagle, T. (2006). Maintenance of *C. elegans*, `http://www.wormbook.org/chapters/www_strainmaintain/strainmaintain.html`.

Waggoner, L.E., Zhou, G., Schafer, R.W. and Schafer, W.R. (1998). Control of alternative behavioral states by serotonin in *Caenorhabditis elegans*, *Neuron* **21**(1): 203–214.

White, J.G., Southgate, E., Thomson, J.N. and Brenner, S. (1986). The structure of the nervous system of the nematode *Caenorhabditis elegans*, *Philosophical Transactions of the Royal Society* **314**(1165): 1–340.

Wu, Y., Luo, Y., Wu, Z., Butko, P., Christen, Y., Lambert, M.P., Klein, W.L. and Link, C.D. (2006). Amyloid-β-induced pathological behaviors are suppressed by Ginkgo biloba extract EGb 761 and ginkgolides in transgenic *Caenorhabditis elegans*, *Journal of Neuroscience* **26**(50): 13102–13113.

Mateusz Kowalski was born in Poznań, Poland, in 1986. He received the M.Sc. degree in electrical engineering from the Poznań University of Technology in 2010. His research work includes the modeling of biological systems and exoskeleton system control. Since 2010 he has been a Ph.D. student in the Institute of Control and Information Engineering at the Poznań University of Technology.

Piotr Kaczmarek was born in Poznań, Poland, in 1979. He received the M.Sc. degree in electrical engineering from the Poznań University of Technology in 2003 and the Ph.D. degree in biocybernetics from the same university in 2009. His research work includes the modeling of biological systems and FES system control. Since 2003 he has been employed at the Institute of Control and Information Engineering of the Poznań University of Technology.

Rafał Kabaciński was born in Poznań, Poland, in 1986. He received the M.Sc. degree in electrical engineering from the Poznań University of Technology in 2010. His research work includes the modeling of biological systems and vein pattern recognition. Since 2010 he has been a Ph.D. student at the Institute of Control and Information Engineering of the Poznań University of Technology.

Robert Sobkowiak works at the Department of Cell Biology, Institute of Experimental Biology, Adam Mickiewicz University in Poznań, Poland. He received the M.Sc. degree in molecular biology from the Adam

Mickiewicz University in 1998, and the Ph.D. degree in plant physiology from the same university in 2003. Currently, his research concerns quantitative analysis of behavior in *Caenorhabditis elegans*, and the molecular and cellular mechanisms of nicotine addiction.

Received: 13 February 2013
Revised: 25 September 2013
Re-revised: 5 February 2014